Optically Mediated Hybridization between Two Mechanical Modes

A. B. Shkarin,[1,*] N. E. Flowers-Jacobs,[1] S. W. Hoch,[1] A. D. Kashkanova,[1] C. Deutsch,[2] J. Reichel,[2] and J. G. E. Harris[1,3]
[1]Department of Physics, Yale University, New Haven, Connecticut 06520, USA
[2]Laboratoire Kastler Brossel, ENS/UPMC-Paris 6/CNRS, F-75005 Paris, France
[3]Department of Applied Physics, Yale University, New Haven, Connecticut 06520, USA
(Received 3 June 2013; published 8 January 2014)

In this Letter we study a system consisting of two nearly degenerate mechanical modes that couple to a single mode of an optical cavity. We show that this coupling leads to nearly complete (99.5%) hybridization of the two mechanical modes into a bright mode that experiences strong optomechanical interactions and a dark mode that experiences almost no optomechanical interactions. We use this hybridization to transfer energy between the mechanical modes with 40% efficiency.

DOI: 10.1103/PhysRevLett.112.013602 PACS numbers: 42.50.Wk, 42.60.Da, 42.81.Wg, 85.85.+j

Optomechanical systems, in which electromagnetic resonators interact with mechanical resonators, offer a platform for studying a wide range of nonlinear and quantum effects. These systems have been studied in the context of quantum-limited detection of forces and displacements, the production of nonclassical states of light, synchronization and chaotic dynamics, and tests of quantum mechanics with massive degrees of freedom [1].

Optomechanical systems are usually modeled as a single optical mode that is parametrically coupled to a single mechanical mode. This simple model accurately describes many experiments; however, real devices invariably consist of multiple optical and mechanical modes. The presence of multiple modes can provide important capabilities, including new types of optomechanical interactions, robust means for detecting quantum effects, and the ability to transfer quantum states between different systems [2–13].

One important class of multimode optomechanical systems consists of devices in which a single optical mode couples to multiple mechanical modes. This situation arises naturally when an optomechanical device with well-separated optical resonances is driven by a single laser beam. Within the usual weak-coupling description of optomechanics, the undriven optical modes are irrelevant, and only the driven mode needs to be considered [14–16]. Mechanical modes, on the other hand, cannot be ignored just because they are not driven. This is because any optical mode can be detuned (to some degree) by the displacement of any of the devices' mechanical modes. As a result, the effective Hamiltonian for such a device will involve one optical mode coupled to many mechanical modes.

In such a system, the motion of a given mechanical mode will modulate the intracavity optical field, which will in turn drive the other mechanical modes. This can be thought of as an optically mediated coupling between the mechanical modes. This intermode coupling can be neglected for mechanical modes whose resonance frequencies are well separated. However, mechanical resonators with some degree of symmetry will have some nearly degenerate modes, and for these modes this coupling can be important.

In this Letter we demonstrate that the optomechanical coupling between one optical mode and two mechanical modes causes the mechanical modes to nearly fully (99.5%) hybridize into bright and dark states. We then transfer classical mechanical energy between the mechanical modes by modulating the hybridization in a classical analogy to Rabi oscillations. The optomechanical hybridization of mechanical modes has been seen previously in a photonic double-nanobeam system [17], whispering gallery-mode resonators [17,18], and nanobeams embedded in a microwave cavity [19]. However, these experiments did not use this hybridization to transfer energy. Two of these devices would have a low transfer efficiency because of a relatively low mechanical quality factor [17] or incomplete hybridization [19]. We estimate that the device in Ref. [18] could transfer energy with reasonable efficiency, but Ref. [18] focused on using the optical force to regeneratively oscillate and synchronize the two mechanical resonators.

The device described here operates in the classical regime. However, in the quantum regime (that is, when the mechanical modes are nearly in the ground state), the fact that the intrinsic mechanical damping rate is small and the intermode coupling is both conservative and strong (in contrast to previous work [17,19,18]) means that it would be well suited for realizing proposals for entangling mechanical modes and creating nonclassical mechanical states [4,5,8,10]. In addition, the long lifetime of the mechanically dark state could be used to store quantum information [17,20].

The device studied here is a "membrane-in-the-middle" optomechanical system composed of a SiN membrane placed in an optical fiber cavity [Fig. 1(a)] [21,22]. The 70 μm long Fabry-Perot cavity is formed between the end faces of two 200 μm diameter single-mode optical fibers. Each fiber face has a concavity with a 300 μm radius of curvature and a dielectric coating that is highly reflective

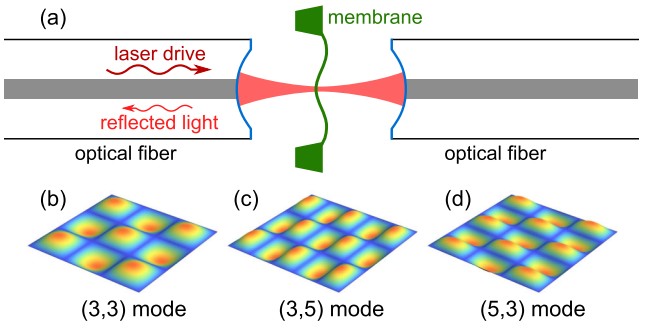

FIG. 1 (color online). (a) Experimental setup with a SiN membrane placed in a cavity formed between the mirrored ends of two fibers. (b)–(d) Schematic representation of the mode shapes of the three relevant membrane modes.

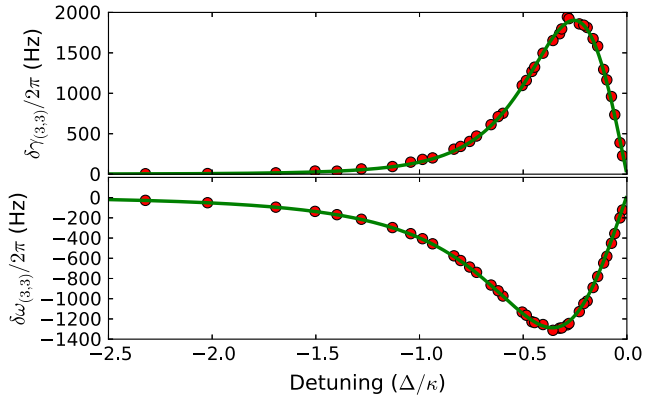

FIG. 2 (color online). Optomechanically induced shift in mechanical linewidth (top) and frequency (bottom) of the (3,3) membrane mode as a function of detuning with theoretical fit (solid green line). These data are taken with an incident power of 3 μW and a cavity linewidth of 21 MHz.

at wavelength $\lambda = 1550$ nm. The resulting cavity has a finesse $\lesssim 100\,000$ depending upon the position of the membrane, corresponding to a cavity linewidth $\kappa/2\pi \gtrsim 20$ MHz.

The SiN membrane is 250 μm square and 100 nm thick. Because it is nearly square and under significant stress, the resonance frequencies of its higher-order modes are expected to be simply related to its fundamental resonance frequency $\omega_{(1,1)}/2\pi = 1.7$ MHz. Labeling each mode by the number of antinodes along each axis (j, k), as shown in Fig. 1, the resonance frequencies are $\omega_{(j,k)} = \omega_{(1,1)}\sqrt{j^2 + k^2}/\sqrt{2}$. We find that the measured $\omega_{(j,k)}$ follow this relationship to within 0.1% for j, $k < 6$, implying that each mode with $j \neq k$ has a (nearly) degenerate partner.

As described in Ref. [22], the membrane is positioned so that the frequency of the optical cavity varies linearly with the membrane position. The cavity is locked to the laser at frequencies $\ll \omega_{(1,1)}$ so the membrane's motion is imprinted on the reflected laser field, which is measured using a heterodyne technique. We measure the power spectral density of the heterodyne signal near the membrane's resonance frequencies and fit these data to extract each mechanical mode's linewidth and resonance frequency.

Before concentrating on the cavity-induced coupling between nearly degenerate mechanical modes, we characterize the optomechanical shift in the resonance frequency ("optical spring") and linewidth ("optical damping") of the nondegenerate (3,3) mode. For this mode, $\omega_{(3,3)}/2\pi = 5.092$ MHz, and the quality factor $Q_{(3,3)} = 500\,000$. The effective mass is $m = \rho V/4 = 5.4$ ng, which is the same for all of the membrane's modes.

The effects of the optomechanical coupling are revealed by varying the detuning Δ between the laser and the cavity. In Fig. 2 we plot the shift in the mechanical linewidth $\delta\gamma_{(3,3)}$ and the resonance frequency $\delta\omega_{(3,3)}$ as a function of Δ. Since $\omega_{(3,3)} \approx 0.2\kappa$ (the unresolved-sideband regime), $\delta\omega_{(3,3)}$ and $\delta\gamma_{(3,3)}$ are largest when $\Delta \approx -\kappa/3$. We separately measure the incident power $P_{\text{in}} = 3$ μW and relative input coupling $\kappa_L = 0.05\kappa$ and fit the data in Fig. 2 to theoretical predictions [14,15] using the single-photon optomechanical coupling $g_{(3,3)}$ and cavity linewidth κ as fitting parameters. The result of this fit is shown in Fig. 2 (green line) and gives $\kappa/2\pi = 21$ MHz and $g_{(3,3)}/2\pi = 1050$ Hz, in agreement with independent measurements.

Now we focus on the effect of the optomechanical coupling on the nearly degenerate (3, 5) and (5, 3) mechanical modes. For these modes, $\omega_{(3,5)}/2\pi = 6.999$ MHz, $\omega_{(5,3)}/2\pi = 7.005$ MHz, $Q_{(3,5)} = 440\,000$, $Q_{(5,3)} = 220\,000$, $g_{(3,5)}/2\pi = 700$ Hz, and $g_{(5,3)}/2\pi = 950$ Hz. In Figs. 3(a) and 3(c) we plot the measured power spectral density of the heterodyne signal as a function of Δ (y axis) and the measurement frequency (x axis) at two different incident powers ($P_{\text{in}} = 3$ μW and $P_{\text{in}} = 38$ μW). The thermal motion of each mode is clearly visible in these power spectral densities.

In order to qualitatively understand the data in Figs. 3(a) and 3(c) and make a comparison with theory, we consider a system of N mechanical oscillators coupled to a single optical mode. This analysis is presented in the Supplemental Material [23]. When $N = 2$, as in our system, we can simplify the more general theory using a description based on bright and dark states.

Specifically, we start with two intrinsic mechanical modes, each with displacement z_n, single-photon optomechanical coupling g_n, intrinsic complex resonance frequency $\xi_n = \omega_n - i\gamma_n/2$, and intrinsic mechanical susceptibility $\chi_n[\omega]^{-1} = i\xi_n - i\omega$ (where $n = 1, 2$). We then define a dark state displacement $z_d = vz_1 - uz_2$, which is a linear combination of the original, intrinsic mode displacements with weights u, $v = g_{1,2}/\sqrt{g_1^2 + g_2^2}$. The "dark" label is used because z_d is not coupled to the cavity (that is, the single-photon optomechanical coupling $g_d = 0$).

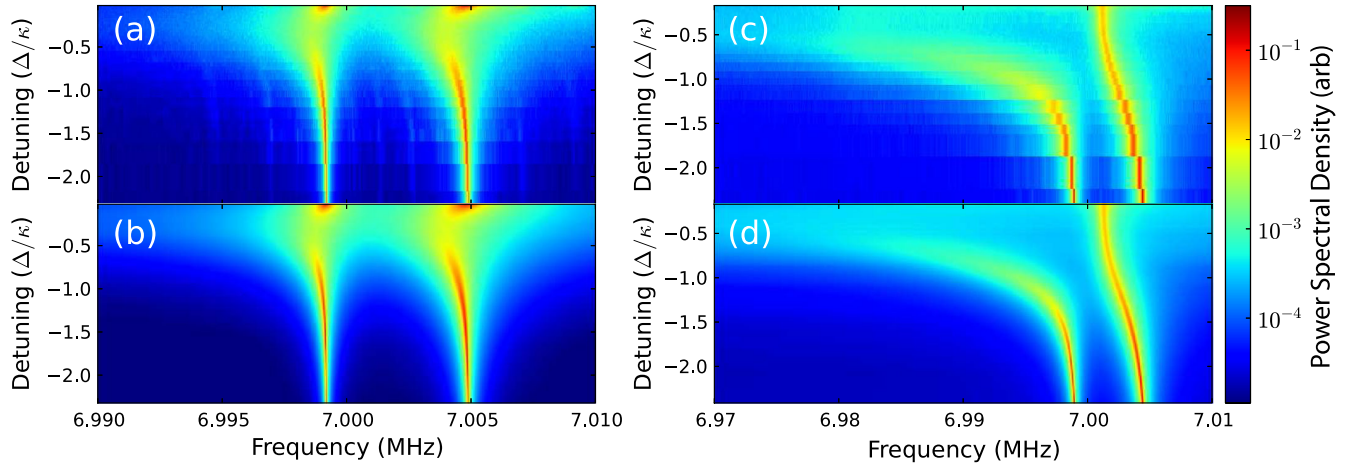

FIG. 3 (color online). Power spectral density (arbitrary units) of the heterodyne signal (a), (c) and theoretical fits (b), (d) as a function of measurement frequency (horizontal axis) and detuning between the incident laser and the cavity resonance (vertical axis). The data are presented for two incident laser powers: 3 μW for (a), (b) and 38 μW for (c), (d). A direct comparison of the theory and the data is shown in the Supplemental Material [23].

On the other hand, the single-photon optomechanical coupling of the bright mode, with modal displacement $z_b = uz_1 + vz_2$, is larger than that of the original modes $g_b = \sqrt{g_1^2 + g_2^2}$. The new modes z_b and z_d have intrinsic complex resonance frequencies $\xi_{b,d} = u^2\xi_{1,2} + v^2\xi_{2,1}$ and are generally not normal modes of the system; the effective coupling between them is $g_{bd} = uv(\xi_1 - \xi_2)$.

Using these expressions, the displacement spectra of z_b and z_d in response to the thermal Langevin forces η_b and η_d are

$$(\chi_b^{-1}[\omega] + i\Sigma_{bb}[\omega])z_b[\omega] = -ig_{bd}z_d[\omega] + \sqrt{\gamma_b}\eta_b[\omega], \quad (1)$$

$$\chi_d^{-1}[\omega]z_d[\omega] = -ig_{bd}z_b[\omega] + \sqrt{\gamma_d}\eta_d[\omega]. \quad (2)$$

The only term in these expressions that depends on the optical drive is the "self-energy" $\Sigma_{bb}[\omega]$, which determines the optical spring $\delta\omega_b = \mathrm{Re}(\Sigma_{bb}[\omega_b])$ and damping $\delta\gamma_b = -2\,\mathrm{Im}(\Sigma_{bb}[\omega_b])$ of the bright mode.

We use this model to fit the data in Fig. 3(a,c) and plot the resulting theoretical curves in Figs. 3(b) and 3(d) (see Supplemental Material for a direct comparison of theory and data [23]). The system parameters κ, Δ, and P_{in} are determined from simultaneous measurements of the (3,3) mode (as in Fig. 2). We then use a least-squared fit to the data in Figs. 3(a) and 3(c) to determine the remaining parameters: $g_{1,2}$, $\omega_{1,2}$, and $\gamma_{1,2}$ [where the subscripts 1 and 2 now label the modes (3,5) and (5,3)].

This model also provides a qualitative interpretation of the data. In order to significantly hybridize the intrinsic modes into bright and dark modes, the optical spring $\delta\omega_b$ needs to be large enough that $|\omega_b + \delta\omega_b - \omega_d| \gg |g_{bd}|$ or, in this case, $-\delta\omega_b/2\pi \gg 1$ kHz. At low P_{in} [Figs. 3(a) and 3(b)] or at high P_{in} and large detunings [near the bottom of Figs. 3(c) and 3(d)], the optical spring is relatively small and this condition is not satisfied. The intrinsic modes do not significantly hybridize and instead independently exhibit essentially the same behavior as shown in Fig. 2 for the nondegenerate (3, 3) mode.

On the other hand, in Figs. 3(c) and 3(d) at detunings $\Delta \gtrsim -1.5\kappa$ the optical spring is large enough that the intrinsic modes begin to hybridize into bright and dark modes. When the detuning $\Delta \gtrsim -0.75\kappa$, the lower-frequency state is almost entirely bright and exhibits large optical spring and optical damping, while the higher frequency state is almost entirely dark (based on the fit parameters from Fig. 3 the hybridization is 99.5%). In this regime the coupling g_{bd} leads to only two noticeable effects. First, it makes the effective dark mode linewidth larger than the intrinsic linewidth of $\gamma_d/2\pi = 20$ Hz. Second, it allows the dark mode to be visible in the reflected light spectrum; otherwise this mode would be completely uncoupled from the cavity field.

The high mechanical quality factors and purely optomechanical coupling of the membrane modes make it possible to observe this hybridization in the time domain. As shown in Fig. 4, modulating the optical drive results in the transfer of mechanical energy between the two intrinsic mechanical modes.

This measurement starts by using a piezo actuator to drive either the (3,5) or (5,3) mechanical mode and locking the cavity to a weak laser beam with detuning $\Delta_{\mathrm{weak}} = -0.7\kappa$ for Figs. 4(a)–4(c) and $\Delta_{\mathrm{weak}} = -0.4\kappa$ for Figs. 4(d)–4(f). For this measurement, the cavity linewidth $\kappa/2\pi = 40$ MHz. The weak laser beam is primarily used to measure the mechanical displacement, though its dynamical backaction does increase the mechanical linewidths by a factor of ~2. The piezo drive is turned off and a strong laser beam at detuning $\Delta_{\mathrm{weak}} + \kappa/8$ and power P_{in} is turned on

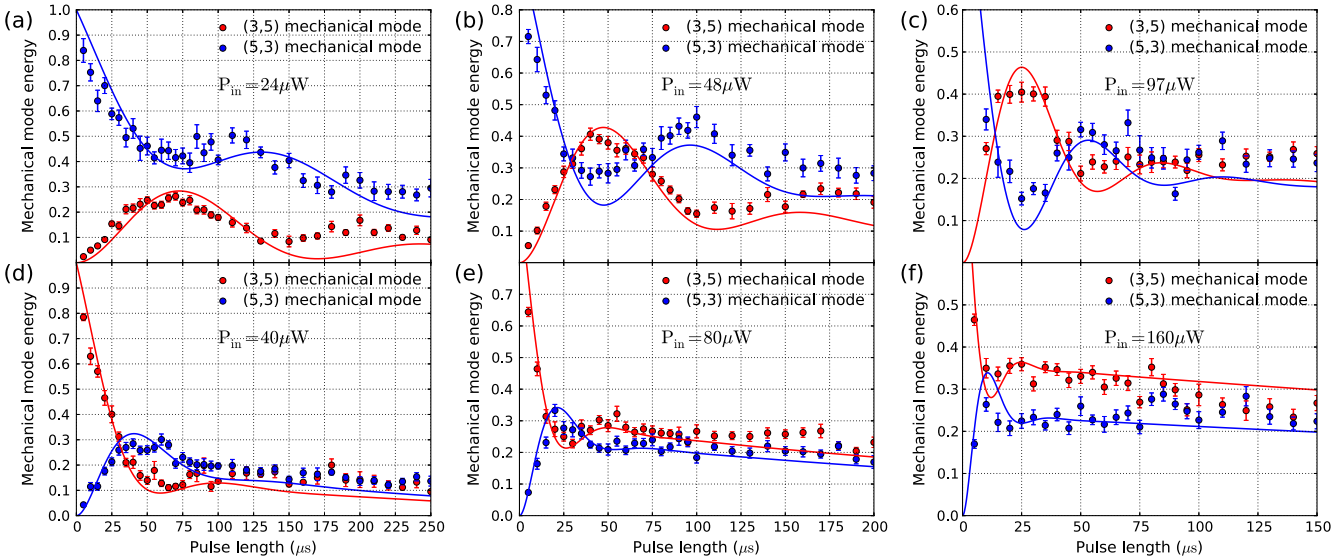

FIG. 4 (color online). The energy in each mechanical mode immediately after a hybridization pulse, plotted as a function of the pulse duration. The energy is normalized to the energy in the driven mode just before the hybridization pulse. In panels (a)–(c) the system is initialized by driving the (3,5) mode and shows the transfer of energy to the (5,3) mode. Panels (d)–(f) show the transfer of energy in the opposite direction. Solid lines are the fits described in the text, and the error bars indicate statistical uncertainties.

for a time τ. This pulse hybridizes the mechanical modes. After this pulse, the weak laser beam is used to determine the energy in each of the intrinsic mechanical modes. This measurement is facilitated by the separation in time scales between the 10 ms lifetimes of the intrinsic mechanical modes, the 100 μs period of the hybridization oscillations, the 140 ns period of mechanical oscillations, and the 10 ns lifetime of the optical cavity.

In Fig. 4 we plot the ratio of the final energy in each intrinsic mechanical mode after the pulse to the total initial energy as a function of τ and at different P_{in}. In Figs. 4(a)–4(c) the system is initialized by driving the (5,3) mode, while in Figs. 4(d)–4(f) it is initialized by driving the (3,5) mode. The theory curves in Fig. 4 are derived from the solution to a set of differential equations describing the motion z_1 and z_2 of two linearly coupled harmonic oscillators. The coupling and oscillator parameters are taken from the self-energy matrix $\Sigma[\omega]$ (see Supplemental Material [23]) and depend on the strength and detuning of the "strong" laser pulse.

In Fig. 4, some of the parameters for the theory curves are chosen manually to match the data. The values of $g_{1,2}$, $\omega_{1,2}$, and $\gamma_{1,2}$ are determined by fitting data similar to Fig. 3. The cavity linewidth κ is measured independently. A single value of Δ_{weak} is chosen to fit the data in the three upper plots. P_{in} is chosen to fit the data in Fig. 4(a), and then increased by a factor of 2 in Fig. 4(b), and another factor of 2 in Fig. 4(c), in accordance with the experimental procedure. The same approach was used to choose different values of Δ_{weak} and P_{in} for the lower three plots. Finally, we apply a scaling factor of 1.3 to the initial energy in the driven mode to correct for the nonlinearity of the detector. This manual choice of five parameters completely determines the theory curves in Fig. 4.

The pulse power used in Fig. 4 is sufficient to hybridize the system, resulting in Rabi-like oscillations between the intrinsic (3,5) and (5,3) eigenmodes. We can gain a more qualitative understanding of the data in Fig. 4 by considering the hybridization of the original modes into bright and dark modes. The oscillation frequency increases with P_{in} since the frequency splitting between the dark and bright modes is increased. The oscillations are suppressed on a time scale given by the optomechanically dominated damping rate of the bright mode, which also increases with increasing P_{in}. After the bright mode decays, the ratio of the energy in the two modes is constant and given by the fractional contribution of each intrinsic mode to the dark mode. The total energy continues to decrease as the dark mode decays.

By optimizing the pulse power and length, we are able to transfer energy between the two intrinsic modes with an efficiency of 40% [e.g., see Figs. 4(b) and 4(c)]. This transfer efficiency is limited by the optomechanical damping of the bright mode $\delta\gamma_b$. Since $\delta\gamma_b$ is comparable to the coupling rate between the mechanical modes, significant energy is lost to the optical field during the energy transfer. The transfer efficiency can be increased by increasing the ratio of the optical spring to the optical damping $\delta\omega_b/\delta\gamma_b$ by, for example, operating in either the resolved $\kappa \ll \omega_m$ or unresolved $\kappa \gg \omega_m$ sideband limit [10].

The main barrier between the present setup and operation in the quantum regime is the 300 K temperature of the

environment. To consider the performance of this system in a cryogenic environment, we note that if it was cooled to 100 mK, it would be possible to laser cool both of the membrane modes to a mean energy of less than one phonon [14,15]. Assuming that $Q_{(3,5)}$ and $Q_{(5,3)}$ increase to 5×10^6 at cryogenic temperatures [24,25], the thermal and optomechanically induced decoherence rates become comparable to the coupling strength between the two mechanical modes. With these assumptions, we estimate the quantum state transfer fidelity to be 10% (see Supplemental Material [23]). We note that the device described here is well suited to cryogenic operation. For example, SiN membranes have been used in a number of cryogenic optomechanical experiments [24,25] and we have shown that fiber cavities can operate at 4 K (see Supplemental Material [23]).

We thank H. Seok and P. Meystre for helpful discussions related to quantum state transfer. This work has been supported by the DARPA/MTO ORCHID program through a grant from AFOSR.

*alexey.shkarin@yale.edu

[1] V. B. Braginsky, Y. I. Vorontsov, and K. S. Thorne, M. Aspelmeyer, T. J. Kippenberg, and F. Marquardt, arXiv:1303.0733v1.
[2] V. B. Braginsky, Y. I. Vorontsov, and K. S. Thorne, Science **209**, 547 (1980).
[3] J. D. Thompson, B. M. Zwickl, A. M. Jayich, F. Marquardt, S. M. Girvin, and J. G. E. Harris, Nature (London) **452**, 72 (2008).
[4] M. J. Hartmann and M. B. Plenio, Phys. Rev. Lett. **101**, 200503 (2008).
[5] C. Genes, D. Vitali, and P. Tombesi, New J. Phys. **10**, 095009 (2008).
[6] P. Verlot, A. Tavernarakis, T. Briant, P.-F. Cohadon, and A. Heidmann, Phys. Rev. Lett. **102**, 103601 (2009).
[7] J. C. Sankey, C. Yang, B. M. Zwickl, A. M. Jayich, and J. G. E. Harris, Nat. Phys. **6**, 707 (2010).
[8] M. Ludwig, K. Hammerer, and F. Marquardt, Phys. Rev. A **82**, 012333 (2010).
[9] C. A. Regal and K. W. Lehnert, J. Phys. Conf. Ser. **264**, 012025 (2011).
[10] H. Seok, L. F. Buchmann, S. Singh, and P. Meystre, Phys. Rev. A **86**, 063829 (2012).
[11] H. Tan, F. Bariani, G. Li, and P. Meystre, arXiv:1302.7087v1.
[12] A. Xuereb and M. Paternostro, Phys. Rev. A **87**, 023830 (2013).
[13] G. Heinrich and F. Marquardt, Europhys. Lett. **93**, 18 003 (2011).
[14] I. Wilson-Rae, N. Nooshi, W. Zwerger, and T. J. Kippenberg, Phys. Rev. Lett. **99**, 093901 (2007).
[15] F. Marquardt, J. P. Chen, A. A. Clerk, and S. M. Girvin, Phys. Rev. Lett. **99**, 093902 (2007).
[16] H. K. Cheung and C. K. Law, Phys. Rev. A **84**, 023812 (2011).
[17] Q. Lin, J. Rosenberg, D. Chang, R. M. Camacho, M. Eichenfield, K. J. Vahala, and O. Painter, Nat. Photonics **4**, 236 (2010).
[18] M. Zhang, G. S. Wiederhecker, S. Manipatruni, A. Barnard, P. McEuen, and M. Lipson, Phys. Rev. Lett. **109**, 233906 (2012).
[19] F. Massel, S. U. Cho, J.-M. Pirkkalainen, P. J. Hakonen, T. T. Heikkilä, and M. A. Sillanpää, Nat. Commun. **3**, 987 (2012).
[20] A. H. Safavi-Naeini, T. P. M. Alegre, J. Chan, M. Eichenfield, M. Winger, Q. Lin, J. T. Hill, D. E. Chang, and O. Painter, Nature (London) **472**, 69 (2011).
[21] D. Hunger, T. Steinmetz, Y. Colombe, C. Deutsch, T. Hänsch, and J. Reichel, New J. Phys. **12**, 065038 (2010).
[22] N. E. Flowers-Jacobs, S. W. Hoch, J. C. Sankey, A. Kashkanova, A. M. Jayich, C. Deutsch, J. Reichel, and J. G. E. Harris, Appl. Phys. Lett. **101**, 221109 (2012).
[23] See Supplemental Material at http://link.aps.org/supplemental/10.1103/PhysRevLett.112.013602 for a more detailed theoretical description and a discussion of possible future measurements in the quantum regime.
[24] A. M. Jayich, J. C. Sankey, K. Borkje, D. Lee, C. Yang, M. Underwood, L. Childress, A. Petrenko, S. M. Girvin, and J. G. E. Harris, New J. Phys. **14**, 115018 (2012).
[25] T. P. Purdy, R. W. Peterson, P. L. Yu, and C. A. Regal, New J. Phys. **14**, 115021 (2012).